Catalysis Today 161 (2011) 97–104

Contents lists available at ScienceDirect

Catalysis Today

journal homepage: www.elsevier.com/locate/cattod

Physical and chemical properties of titanium dioxide printed layers

Marcela Černá, Michal Veselý, Petr Dzik*

Brno University of Technology, Purkynova 118, 612 00 Brno, Czech Republic

ARTICLE INFO

Article history:
Received 21 June 2010
Received in revised form 12 October 2010
Accepted 7 November 2010
Available online 10 December 2010

Keywords:
Titanium dioxide
Sol–gel
Inkjet printing
Cracking
Polyethylene glycol

ABSTRACT

This study focuses on the preparation of the TiO_2 thin films from alkoxide solutions containing polyethylene glycol (PEG) as an anticracking agent by the sol–gel method on soda–lime glass plates. Sol application was carried out by inkjet printing using a modified office inkjet printer equipped with piezoelectric print head. The grey level of the printed image was varied in order to control the sol loading of the resulting printed pattern. The effect of PEG addition on the precursor and prepared layer properties was studied. Also, the influence of sol loading on physical properties and on photocatalytic activity of the printed layers was investigated. The thickness of prepared layer was studied by NanoCalc 2000 and the structure of prepared layers was evaluated by optical microscopy, AFM and SEM. The hydrophilic properties of TiO_2 thin films were studied by examining the contact angle of water on these films. Photocatalytic activity was investigated as a rate of 2,6-dichloroindophenol (DCIP) decomposition. In all cases, we prepared transparent thin layers of TiO_2 with varying thickness and surface morphology. PEG proved to be an efficient agent suppressing the formation of cracks.

1. Introduction

Photoinduced processes are studied in a manifold ways and various applications have been developed since their first description. Despite the differences in character and utilization, all these processes have the same origin. Semiconductors can be excited by radiation of higher energy than the band gap and an energy rich electron–hole pair is formed. This energy can be utilized electrically (solar cells), chemically (photochemical catalysis), or to change the catalyst surface itself (super-hydrophilicity).[1]

We concentrate on titanium dioxide, TiO_2, which is one of the most important and most widely used semiconductors. TiO_2 has received a great deal of attention due to its chemical stability, nontoxicity, low cost, and other advantageous properties. As a result of its high refractive index, it is used as anti-reflection coating in silicon solar cells and many thin-films optical devices [2].

TiO_2 can be deposited on a variety of substrates, such as glass, ceramics or metal panels. During the past two decades, many synthetic methods have been proposed to obtain mesoporous titanium dioxide including the sol–gel method, template method, hydrothermal method, solvothermal method, ultrasound-induced method, ion liquid method, and evaporation-induced self-assembly method [3–10]. Particularly, it has been reported that materials prepared by the sol–gel process are more bioactive than materials of the same compositions but prepared by other methods [11]. At the same time, templating has become one of the most attractive methods used to obtain porous structure [12]. In this work we prepared thin TiO_2 layers by inkjet printing. This method is quite attractive since it provides a great level of control over the layer formation process and the possibility to tune the composition of deposited films [13].

The photocatalytic activity of resulted TiO_2 film depends strongly on the crystal phase structures, thickness and porosity of the thin films. A highly porous surface structure is very imperative among these factors because it offers a much larger number of catalytic sites than a dense surface.

Porous inorganic TiO_2-anatase films can be obtained using templating membranes or conventional alkoxide sol–gel route with the addition of surfactants [14]. The templates permit to retain the initial polymer morphology up to the final porous structure. Polyethylene glycol is especially suitable for modifying the porous structure of coatings [15] due to its complete decomposition at relatively low temperature [16]. To prepare porous and thicker TiO_2 films, Miki et al. had developed the new precursor solution comprised of aqueous TiO_2 sol and PEG, into which trehalose dehydrate was added as a viscous solvent [17]. In this study, PEG functioned as a pore-forming agent. Kajihara and Nakanishi prepared thicker TiO_2 macroporous films from a system containing PEG and poly(vinylpyrrolidone) (PVP), where PEG also played the role of pore-forming reagent and PVP having higher molecular weight was used to increase the viscosity of the solution [18]. The formation of porous structure in TiO_2 thin films strongly depends on the amount and the molecular weight of PEG [19].

In recent studies, several authors reported that the introduction of PEG enhances the crystallite size while it reduces density of the crystallite compared to the TiO_2 film of the same thickness,

* Corresponding author. Tel.: +420 541 149 411; fax: +420 541 211 697.
E-mail address: petr@dzik.cz (P. Dzik).

0920-5861/$ – see front matter © 2010 Elsevier B.V. All rights reserved.
doi:10.1016/j.cattod.2010.11.019

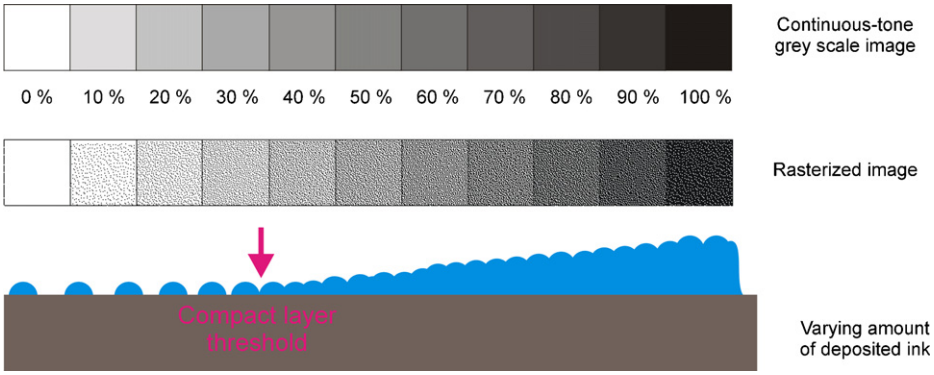

Fig. 1. Layer build-up for different values of sol loading.

prepared without PEG. It was also observed that PEG induced modification is a gradual change from dense, random structure to an early stage of porous network structure, where porosity and roughness increases continuously [20]. With increasing amount of added PEG also the hydroxyl group content of TiO_2 thin films increase and after adding suitable amount of PEG the photoinduced superhydrophilicity can be enhanced and it can caused forestalling of the conversion from the hydrophilic to the hydrophobic state [21].

However, the aim of this work was to investigate the photocatalytic activity of compact, nonporous TiO_2 thin films prepared with the addition of PEG as an anticracking agent.

2. Experimental

2.1. Synthesis of sol

The titanium dioxide sol was prepared using titanium(IV) isopropoxide (TTIP, p.a. purity, Fluka, Germany) as a precursor by the following route. Firstly, 40 mL of absolute ethanol (p.a., Penta, Czech Republic) was mixed with 3.8 mL of acetyl-acetone (p.a., Lachema, Czech Republic). This prepared mixture was added dropwise to TTIP under continuous stirring to control the hydrolysis and condensation reactions. This solution was maintained for a few minutes to obtain the complex chelate. Then absolute ethanol (45 cm^3) with 0.69 cm^3 of water was added drop by drop to the prepared mixture to start the hydrolysis and condensation reactions. Different amounts of PEG (p.s., Merck, Germany) with average molecular weight of 1500 were added to form the printing solutions (0, 1, 4, 16 g/L). Sol was the stored in darkness at the temperature 5 °C for a several days before it was deposited by inkjet printing.

The viscosities of prepared solutions were measured by automatic viscosimeter AVMn (Anton Paar). We observed a viscosity change as a function of the amount of present PEG. The densities were measured by densitometer DMA4500 (Anton Paar) and also in this case we observed the dependence of PEG amount on the results density. All measurements were performed at the temperature of 25 °C.

2.2. Coating deposition

Soda–lime glass plates with size 50 mm × 50 mm × 1.1 mm were chosen as substrates for the immobilization of TiO_2 thin films. Firstly, the glasses had to be pre-tread in sulphuric acid (50%, for 120 min) in order to prevent sodium ions diffusion, which would have caused a reduction of photocatalytic activity [22]. Subsequently, these plates were washed in a surfactant solution to remove of dust, grease and other residues, which might have collected during the storage of pre-treated glass plates.

Sol application was carried out by a novel innovative way utilizing a modified office inkjet printer (Epson R220). Firstly all original cartridges were removed and the ink tubing and printhead were purged by anhydrous propanol. This step is very important for removing any traces of remaining aqueous ink because if the sol came in contact with aqueous impurities the precipitated TiO_2 would clog the printhead nozzles.

Then the prepared sols were filtered through 0.45 μm mesh size syringe filter into the one of the ink cartridges, the other remained empty. The full cartridge was installed into the printer in the black position. After a series of head cleaning cycles a perfect nozzle check pattern was obtained. Since the sol is essentially colorless when viewed in daylight, the nozzle check printout had to be observed under a UV-A light source to prove all ink nozzles of the black channel were firing the loaded sol. Under this type of illumination, the printed sol appeared deep yellow while the paper was bright blue because of fluorescent brightening agents present in the paper [23]. Then the glass substrates were mounted into a modified CD holder, fed into the printer and printed with “black only” driver setting. It means that only the ink from the “black” cartridge (now containing titanium sol) was utilized for printing.

One of the inherent advantages of this method is that we can directly control the amount of the deposited sol (i.e. the sol loading) by changing the grey-scale level of the printed image. In Fig. 1 we can observe the creation of printed layer. The different grey levels (generally continuous tone bitmap) need to be converted into a halftone screen patter (planar distribution of dots). In the case of inkjet printing, a combination of amplitude modulation screening and frequency modulation screening is used: ink droplets of varying size are placed at different pitch. However, printing on non-porous, non-absorbing substrates results into a very high level of dot gain (the printed droplets spread on the substrate and their diameter is much larger than diameter of eject droplet which roughly corresponds to the nozzle diameter). Therefore, the printed substrate becomes completely covered by the ink at lower tonal vales (the compact layer threshold, see Fig. 1). Before this point, the substrate is covered by separate individual droplets. Beyond this point, the substrate is covered by varying amount of ink resulting into a compact layer of varying thickness.

In this work, three levels (100%, 90% and 80%) were used to give samples having three different thicknesses. Before the printing we had to also choose from three modes of the printer operation – “Slow, Medium and Rapid” [22]. Mode “Rapid” was chosen in this work. This mode means that the printhead runs very quickly above the glass surface and it prints continuously in both directions. Because the motion of the printhead and the sol deposition is very fast, the evaporation of the printed solutions takes after the printing phase is finished. Hence, in this way smooth and glossy layer of TiO_2 can be obtained.

Finally, the deposited layers were dried in an oven at temperature 110 °C for 30 min and consequently they were thermally treated in a calcinations furnace at 450 °C for 4 h with the ramp of 3 °C/min.

2.3. Characterization of prepared layers

The thickness of prepared thin films was determined by specular reflectance measurements using NanoCalc-2000 (Micropack, Germany). This method is based on the evaluation of how the film interacts with light. The main advantages of this method are accuracy, high speed, simplicity, non-destructive approach and no need of sample preparation.

The quality of prepared layers was investigated by optical microscope Nikon Eclipse E200. The records were obtained from a digital camera Nikon D70 mounted on the optical microscope. The influence of PEG and the sol loading on a cracking intensity were evaluated from the optical images.

The surface topology was studied by atomic force microscopy AFM. Veeco Di CP-II (Dymek, Japan) machine in a tapping mode was used for this purpose. SEM imaging was performed in Hitachi S4700 FESEM scanning electronic microscope.

The crystalline composition of TiO_2 thin films was determined by Raman spectroscopy. For this purpose we used LabRAM HR Jobin-Yvon Raman spectrometer. The argon–krypton laser RM 2018 (Spectra Physics) at 514.5 nm was used as the excitation source and laser power was kept at 1 mW.

The hydrophilic properties of prepared layers were studied by examining the contact angle of water on TiO_2 thin films. The determination was performed on the OCA20 (Dataphysics, Germany) by applying a sessile drop method. After the droplet deposition, its evolution was recorded by a CCD camera and the contact angle was obtained by the software processing the tangent method. Water droplets were placed at five different positions for one sample and average value was adopted as a contact angle. We investigated by this method, freshly prepared layers and also films, which were placed in the darkness for 10 days.

2.4. Photocatalysis

Photocatalysis experiments were performed in an aqueous solution of 2,6-dichloroindophenol (DCIP) with an initial concentration of 2×10^{-5} mol/L. The photocatalysis reactor consists of two beakers, which were connected by a peristaltic pump. The samples were placed in one of the beaker and the other beaker was used a storehouse for DCIP. The UV irradiation was provided by high-pressure mercury lamp (OSRAM HQL 125W). This lamp had the same distance from the sample for all experiments. The intensity of UV light was 10 W/m^2 and it was measured by X97 Irradiance Meter with X9-7 probe.

A water cell was used to remove IR radiation. Before the reaction, each glass plate was irradiated for 10 min and then 2 mL of reaction solution was sampled every 5 min for UV–vis analysis.

3. Results and discussion

3.1. TiO_2 sols and films

Transparent thin films of photocatalytic TiO_2 were prepared using the sol–gel method. The sol was deposited onto the soda–lime glass plates by inkjet printing, gelled at 110 °C and calcinated at 450 °C. Four different concentration of PEG (0, 1, 4 and 16 g/L) denoted PEG 0, PEG 1, PEG 4, PEG 16 and three sol loadings (100%, 90% and 80%) were used.

The prepared sols were characterized by the investigation of their viscosity and density. Viscosity was measured during 17 days

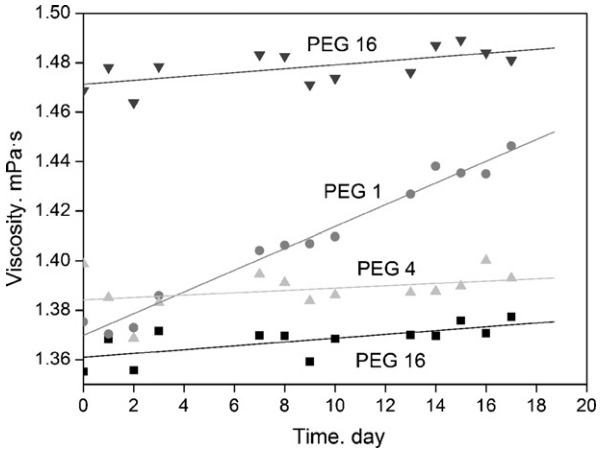

Fig. 2. Change of viscosity during 17 days.

Table 1
Density of prepared sols.

Type of sol	Density (g/mL)
PEG 0	0.8193
PEG 1	0.8196
PEG 4	0.8208
PEG 16	0.8263

because it was the maximal time for which all sols were stored before printing. We examined if the rheological properties are modified during this time. It was discovered that the viscosity was varied insignificantly (Fig. 2). From these results it was concluded that all sols can be stored for this time without change of their rheological properties.

After comparing the density of the solutions it was discovered that the density increases with increasing amount of PEG in samples. The exact values can be found in Table 1.

3.2. Characterization of prepared layers

We probed the dependence of PEG amount and sol loading on the final thickness of TiO_2 layers. It was discovered that there is not

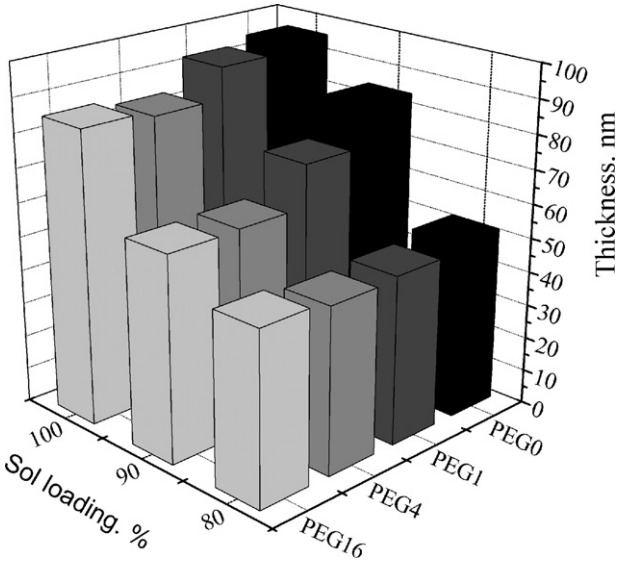

Fig. 3. The dependence of thickness of thin layers on the PEG amount for different sol loading.

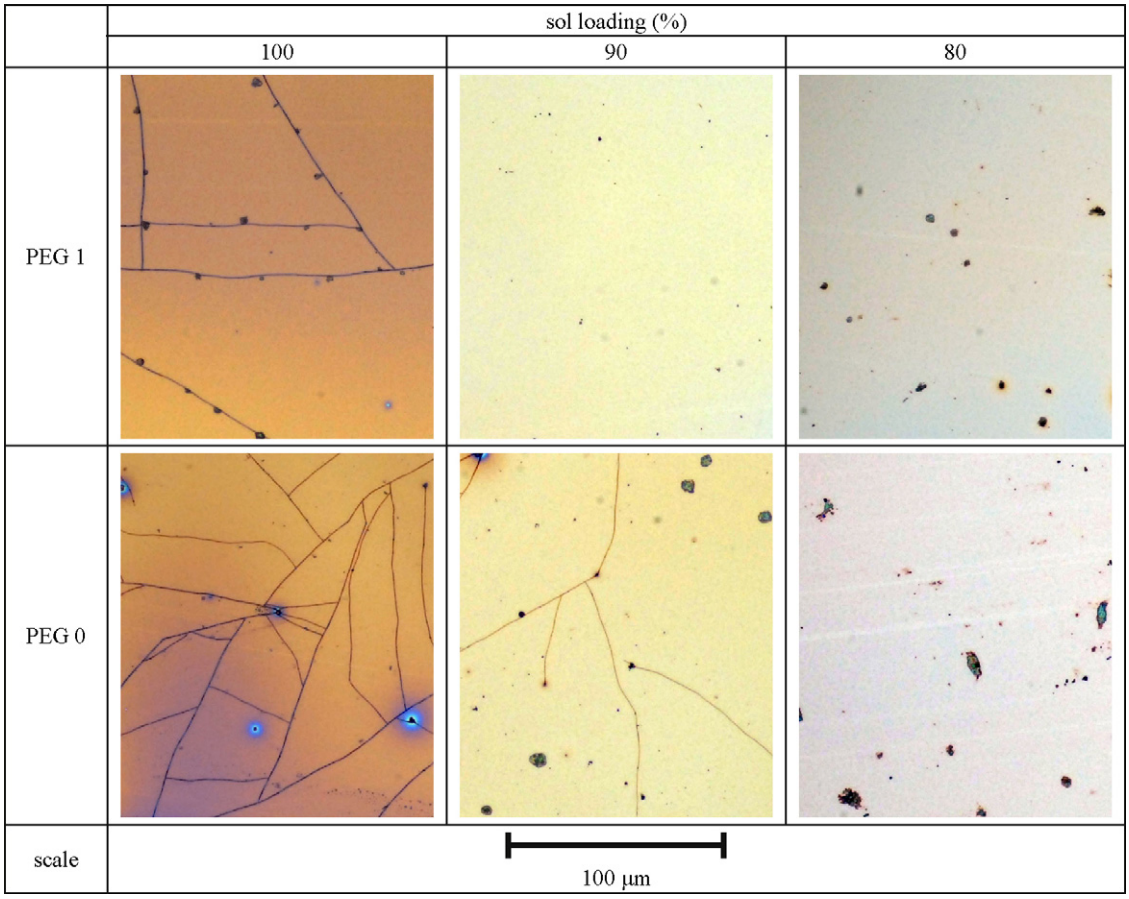

Fig. 4. The influence of sol loading on the cracking intensity.

a great difference between the samples PEG 0 and PEG 1. On the other side, there is a notable decreasing in the thickness for PEG 16 apparently caused by the removal of the organic matrix. With added PEG the viscosity is naturally changing. An increase of the viscosity would have a significantly influence in dip-coating and spincoating. However, based on our experience, the observed change of the viscosity does not affect the layer thickness of inkjet printed layers. Within the studied viscosity range, the droplets are formed in the same way, their amount and most important their volume is constant, so also the thickness of printed layer has to be independent on viscosity (but influenced by the organic matrix franction content). We also confirmed that with increasing sol loading the thickness of prepared TiO_2 layers increase. So the highest value was reached in 100% sol loading (Fig. 3).

The quality of prepared layers was investigated by optical microscopy. All samples were optically transparent and they adhered well to the glass substrate after the calcinations process. We found out that as the sol loading decreases (i.e. the layer thickness), so does the amount of cracks (Fig. 4). In case of 80% there were no cracks present. This cracking is caused by a tensile stress, which arises during the thermal treatment of layers.

When PEG was added to the sol, it induced a gradual suppression of cracking (Fig. 5). All cracks disappeared when the concentration of PEG reached 4 g/L. This was observed in all prepared samples.

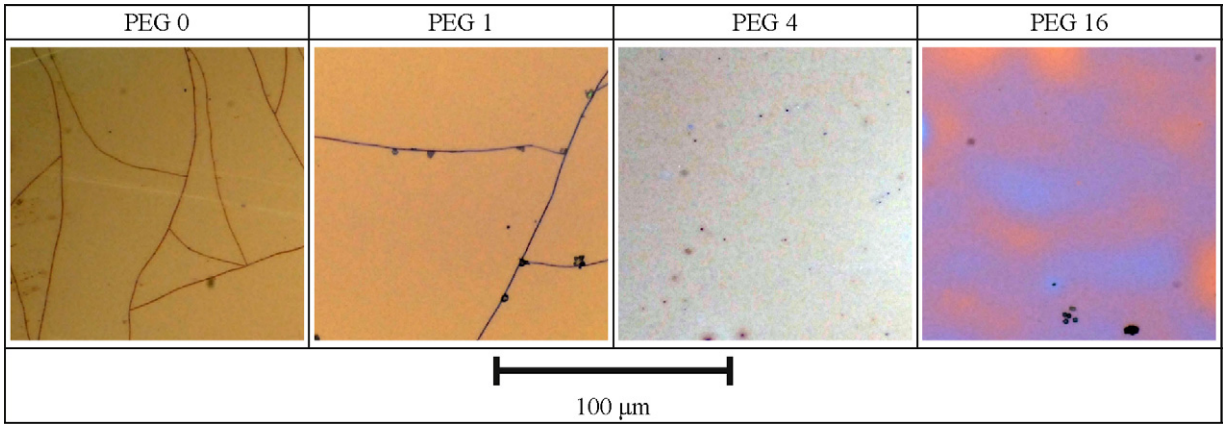

Fig. 5. The influence of PEG on the cracking intensity.

We believe the free volume created by PEG decomposition enables the stress-free arrangement of TiO_2 crystallites created during the calcinations step and in this way the formation of cracks is suppressed.

The surface topology was further studied by AFM microscopy. The influence of added PEG on the roughness of prepared films was evaluated. The results can be observed in Fig. 6. When we compare the roughness for the sample PEG 0 and PEG 16 (see the vertical scale) we can conclude that the roughness increases with increasing amount of PEG in the samples.

The SEM images (Fig. 7) give us a detailed look at appearance of the printed layer at the nanoscale. We can roughly estimate the size of primary crystallites to be approximately in the range of 30–50 nm. We can also clearly see that the way the primary cracks develop at the nanoscale is different: with the addition of PEG, the primary nanocracks are shorter and more frequent. We assume this contributes to better relaxation of tensional stresses occurring during the calcination of the layer and thus prevent the formation of larger microcracks. We also studied the thickness of the layers (Fig. 8) and we compared these results with results from specular reflectance measurement. Generally, we obtained higher values of thickness from SEM then from the optical measurement

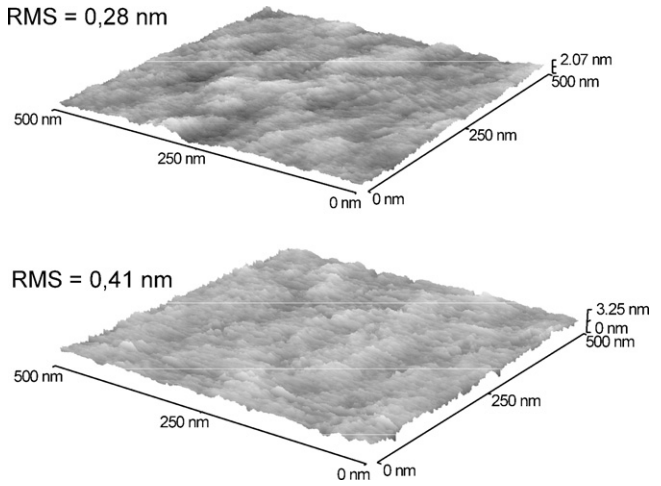

Fig. 6. The influence of PEG on the roughness of thin layers of PEG 0 (left) and PEG 16 (right).

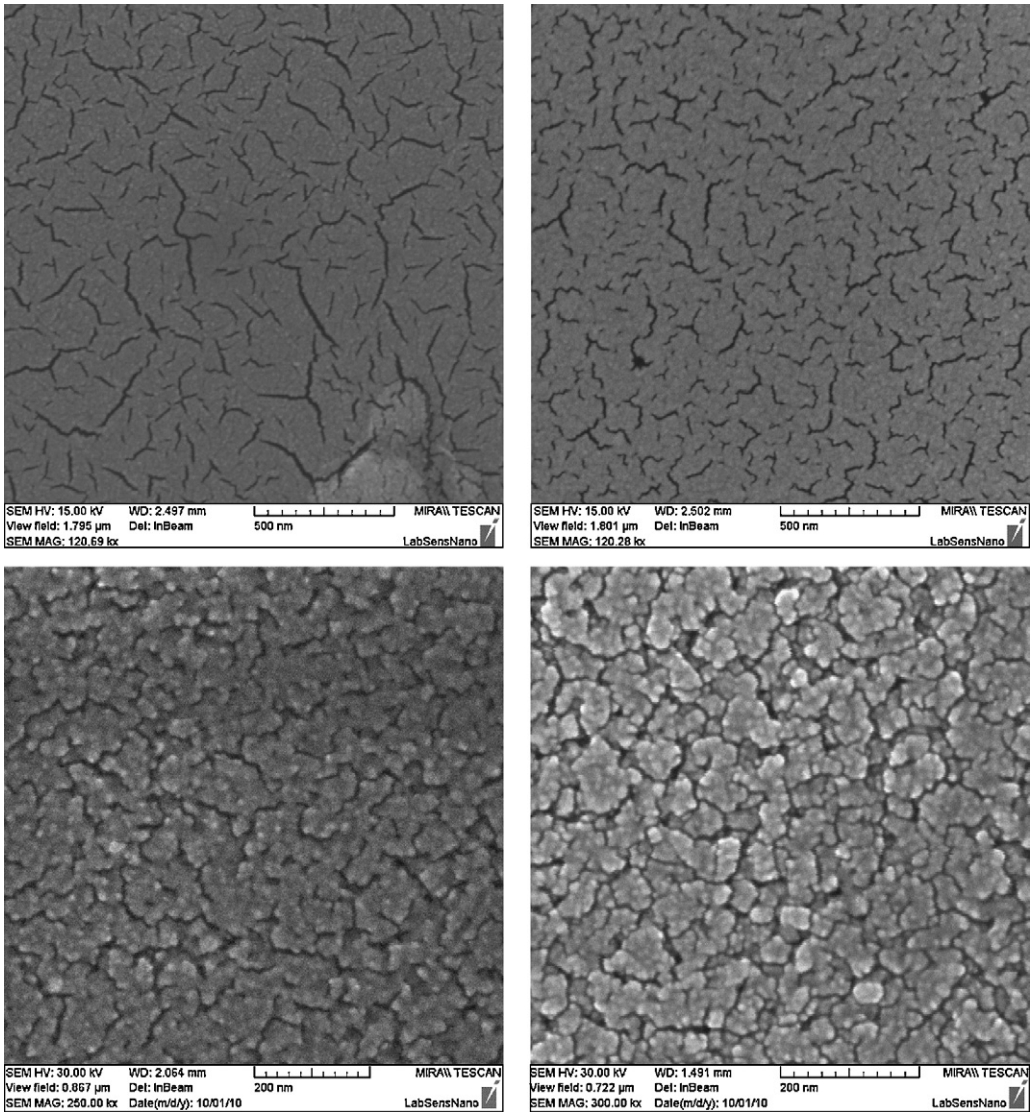

Fig. 7. SEM of the surface of TiO_2 thin films of PEG 0 (left) and PEG 16 (right).

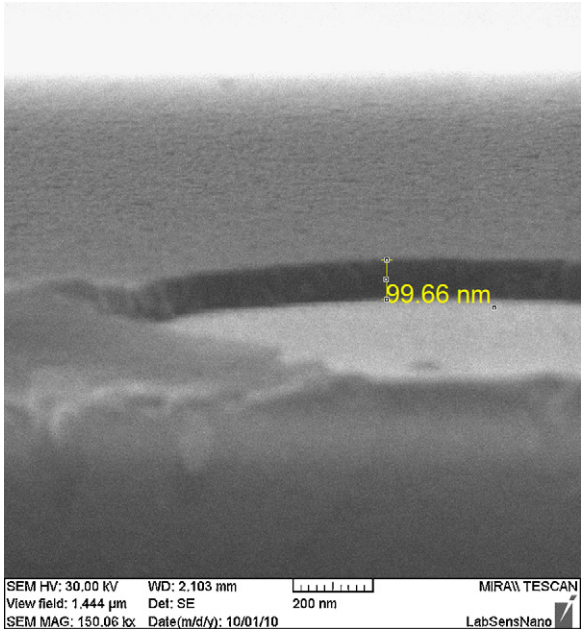

Fig. 8. Thickness of PEG 4 by SEM.

by NanoCalc. We believe this difference is caused by the porosity of prepared layers: Values from SEM give the real geometrical thickness of the layer, including voids, while the results from optical measurements give the net optical thickness of TiO_2 interacting with the probing beam. Of course, the actual refractive index porous layers will be lower then refractive index of bulk TiO_2. Also, other phenomena such as surface roughness may influence the results obtained from the optical method. Anyway, the optical measurement gives us a very easy way of comparing the relative thicknesses of studied layers.

Raman spectroscopy was employed to reveal the crystalline structure of prepared layers. In this particular case, the printed samples were compared to a dipcoated samples prepared using the same sol in order to see if the hydrodynamic stresses during printing have any impact on the crystalline structure of resulting TiO_2 (Fig. 9). It has been described that TiO_2 has 4 active Raman modes in rutil phase, (A_{1g}, B_{1g}, B_{2g} and E_g), 6 for anatase (A_{1g}, $2B_{1g}$ and $3E_g$) and 36 for brookite (61, 62). Indeed, Raman spectra can be influenced by chemical and structural defect causing shift in Raman band positions. Recorded spectra of the sol–gel originated TiO_2 (both printed and dip-coated) were compared with the spectrum of Degussa P-25 as the *de-facto* industrial standard of photocatalytic

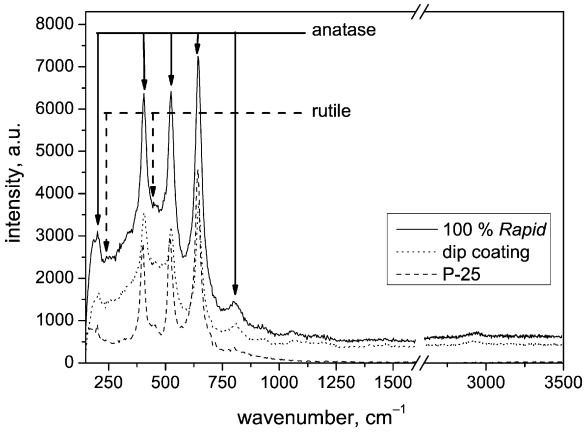

Fig. 9. Comparison of Raman spectra of Degussa P-25, dipcoated and printed sample.

Table 2
Raman bands identification.

Phase	P-25 [cm^{-1}]	dip-coating, 2 layers (84 nm) [cm^{-1}]	100% rapid printing [cm^{-1}]	Vibration mode
Anatase	197	201	201	E_g
Rutile	–	240	240	–
Anatase	401	401	401	B_{1g}
Rutile	444	436	436	E_g
Anatase	517	521	521	A_{1g}, B_{1g}
Anatase	642	642	646	E_g
Anatase	800	807	803	B_{1g}

TiO_2. Our spectra confirmed the presence of anatase phase with a small portion of rutile [23] (Table 2).

The hydrophilic properties of prepared layers were evaluated by measuring the water contact angle as a function of the incident UV light exposure dose. All freshly prepared films showed hydrophilic properties. However, after placing these samples to the darkness for 16 days, we found out that the contact angle grew up in all studied thin films. For example, the contact angle for water on the PEG 1 grew up to 50° after 16 days in the darkness. Obviously, after the irradiation of these films by UV light with intensity of radiation of 15 W/m^2 all samples were converted hydrophilic nature again.

This could be explained by two ways. One of them is that by UV illumination the holes are transferred to the surface, creating oxygen vacancies most likely at the two coordinated bridging sites, which are suitable for dissociative water adsorption. Photoproduced electrons are also transferred to the surface Ti^{4+}, forming Ti^{3+} followed by the electron transfer to adsorbed oxygen molecules. [24,25]

But on the other site, recent communication by Yates and coworkers suggest that photoproduced hydrophilic behaviour on TiO_2 does not involve the production of surface oxygen vacancy defect sites, enhanced surface Ti–OH coverage on defect sites, or the modified surface bonding of bridging >OH groups. They explain the hydrophilic properties as the production of the critical surface condition at the perimeter of a water droplet, which covers a hydrocarbon-coated TiO_2 surface. And they discovered that gas-phase O_2 is necessary to cause the photoinduced hydrophilicity effect. [26]

Recently, it had been found that the contact angles for water on the porous TiO_2 films decreased with increasing of PEG [27]. This has been confirmed by our experiment: samples PEG 0 had the greatest contact angles. It could be caused by a smaller hydroxyl group content and smaller surface roughness since in this case water could not easily enter the interior region of the thin films. Previous studies report that larger amount of the added PEG caused higher roughness so also larger surface area. The coating films with larger surface area are more easily attacked by the water vapour to produce more hydroxyl groups. Hydroxyl groups existing in the coating films are attributed to the chemically adsorbed H_2O and also some H_2O is physically adsorbed on the surface of TiO_2 coating films. Generally, with the increase of chemically adsorbed hydroxyl groups on the surface, van der Waals forces and hydrogen bonds interactions between water and hydroxyl groups will be increased. Water can easily spread across the surface and the hydrophilic character will be enhanced [27].

The rate of conversion from hydrophobic to hydrophilic character of prepared layers was studied. In order to evaluate the contact angle changes upon UV irradiation, the relative change of contact angle has been plotted as a function of the irradiation time. The relative plot has been adopted to be able to compare the samples with different PEG content which showed different values of initial contact angle.

The smallest rate was observed for the samples PEG 0. On the other side, the highest value of conversion rate was observed in

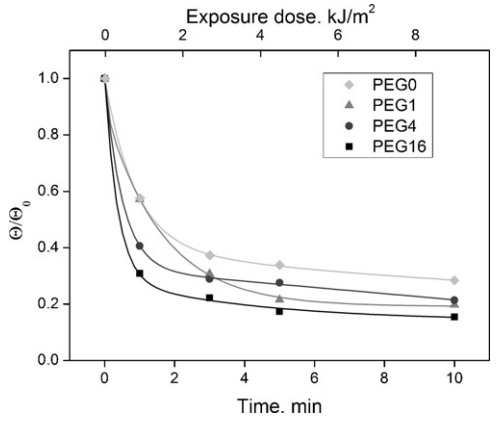

Fig. 10. Decreasing of water contact angle after 10 min of irradiation.

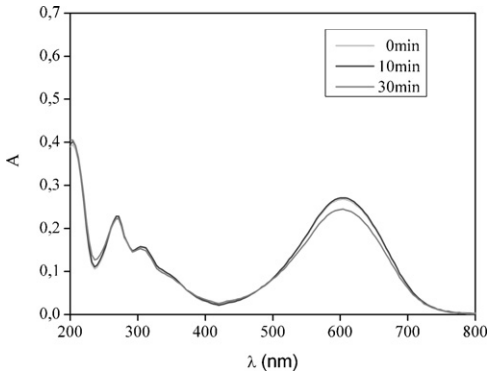

Fig. 11. Change of the absorption spectra of 2,6-dichloroindophenol during 30 min (blank).

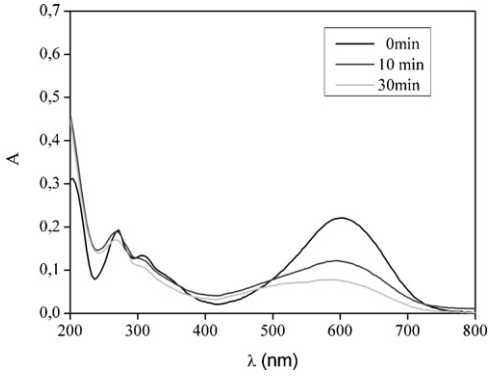

Fig. 12. Decreasing absorbance with irradiation time (PEG 16).

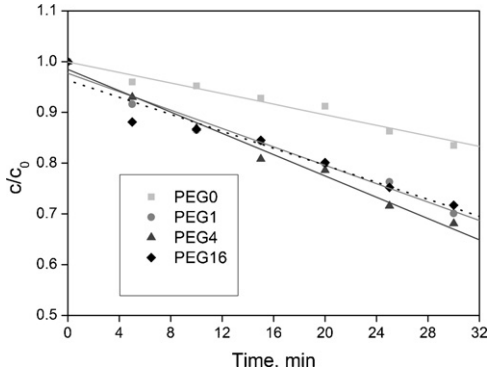

Fig. 13. Decreasing of 2,6-dichloroindophenol during first 30 min.

sample PEG 16 (Fig. 10). It can be explained by the different roughness of the samples, as the PEG 16 sample reached higher roughness (0.50 nm) than PEG 0 sample (0.32 nm).

3.3. Photocatalysis

The photocatalytic activity was evaluated as a rate of DCIP degradation realized in a batch reactor. The first step of the degradation is dechloration accompanied by discoloration. Then, the oxidation of carbon skeleton follows, leading to the creation of short carboxylic acids. Finally, these acids undergo decarboxylation and are totally cleaved. [28–30] The discoloration is naturally very easy to measure by UV–vis spectroscopy. This is very attractive from the practical point of view as inexpensive instrumentation can be used for the studying of photocatalytic efficiency. However, the authors are well conscious of the problems inherently associated with using any dye molecule for the photocatalytic testing: dye molecules can absorb photons, especially in the visible light range, and thus photoexcited electrons may be injected into the conduction band of TiO_2, and the dye is thereby oxidized. [31,32] From the scientific point of view, using simple molecules such as formic acid or dichloroacetic acid make much more sense [33].

Nevertheless, DCIP was chosen due to its very easy detection in the VIS range and a very low absorption at 360 nm wavelength. Moreover, an experiment with a blank (without photocatalyst) was carried out (Fig. 11). There was a little (up to 10%) decrease of absorbance of the blank due to direct photolysis. This value was subtracted from the final measured values to obtain the net photocatalytic efficiency.

DCIP has an absorbance maximum at 600 nm Fig. 12, the reduction rate of which reflects the photocatalytic reactivity of TiO_2 upon UV irradiation. The total reaction time for photocatalytic test was 30 min as this time was sufficient for a total decolorization of DCIP.

In Fig. 13 we can observe the profiles of the time-dependent photocatalytic reactivity of different TiO_2/PEG thin films. As we can observe, the absorbance of treated DCIP solution at 600 nm decreases with the irradiation time. We compared the photocatylytic efficiency of samples with and without PEG. We discovered that samples with PEG have higher photocatalytic activity than the sample without PEG. It can be accounted for the higher roughness of thin layers surface, which is created by the present of PEG.

Since the dependence of relative concentration on time is linear within the studied range, we assumed the zero order kinetics model for this part of the reaction coordinate. Therefore, the reaction rate is independent on the substrate concentration. It seems

Table 3
Rate constant and their standard errors.

	80%		90%		100%	
	k ($\times 10^{-8}$), min^{-1}	SE ($\times 10^{-8}$), min^{-1}	k ($\times 10^{-8}$), min^{-1}	SE ($\times 10^{-8}$), min^{-1}	k ($\times 10^{-8}$), min^{-1}	SE ($\times 10^{-8}$), min^{-1}
PEG 0	0.88	0.13	0.89	0.07	0.89	0.07
PEG 1	1.79	0.11	1.70	0.12	1.54	0.13
PEG 4	1.41	0.22	1.64	0.08	1.82	0.06
PEG 16	1.28	0.06	1.30	0.15	1.85	0.20

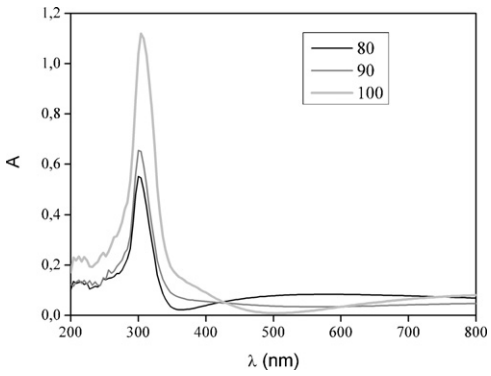

Fig. 14. UV–VIS absorption spectra for layers with different sol loading.

that the rate-determining step is therefore of other nature, such as the rate of electron–hole generation or the substrate delivery and/or removal from the catalyst interface. We calculated the reaction rate constants (k) and their standard errors (SE) for all prepared layers (Table 3).

Then we compared the influence of sol loadings on the photocatalytic reactivity of TiO_2 thin layers. We discovered that the samples with 100% sol loading were the most photocatalytically active. It can be explained by the effect of layers thickness, which is directly related to the value of sol loading.

Generally, when we consider a TiO_2 layer of sufficient thickness (100% layers), a complete absorption of incident radiation can be assumed. In this case, we can see a correlation between the initial drop spreading rate and the rate constants both as functions of PEG content: as the PEG content increases, both the rates increase as well. We assume that similarly to the situation with droplet spreading rate, the addition of PEG increases the surface RMS roughness, which also contributes to the increase in photocatalytic activity.

Such correlation was not observed in the case of thinner layers (80% and 90%). In this case, we do not see any direct influence of the PEG content or layer thickness on the reaction rate. We discovered that in this case the absorption of incident radiation is not complete (Fig. 14). Naturally, the efficiency of absorption can be influenced by other phenomena not identified in this study.

4. Conclusion

Transparent TiO_2 thin films were successfully prepared using PEG in a sol–gel system. The PEG plays a key role in stopping the generation of cracks in the layers during the annealing step at a high temperature. Sol coating on the substrate was performed in a novel way utilizing a modified office inkjet printer. This method often called “material printing” is very efficient, clean and superior to the traditional methods of spin- and dip-coating.

We discovered that the PEG concentration of 4 g/L is sufficient for suppressing the formation all cracks in the layers. When we compared the samples with and without PEG, we found out that with increasing amount of PEG the contact angle is decreasing and so is the value of its initial rate of droplet spreading. It is probably caused by increasing of the roughness with higher PEG concentration. Sample PEG 4 showed the best photocatalytic efficiency. When we compared different sol loading we discovered that the best sample is with 100% sol loading. In the case of thinner layers, the absorption of incident radiation was probably not complete and therefore no general trends were identified.

Acknowledgements

Authors thank to Ministry of Education, Youth and Sports of Czech Republic for support by project OC10050 and the Czech Science Foundation for support through project 104/09/P165.

References

[1] O. Crap, C.L. Huisman, A. Reller, Prog. Solid State Chem. 32 (2004) 33–177.
[2] H.A. Macleod, Thin Film Optical Filters, 2nd ed., Macmillan, New York, 1986, p. 370.
[3] R. Tan, Y. He, Y. Zhu, B. Xu, L. Cao, J. Mater. Sci. 38 (2003) 3973.
[4] C. Wang, Z. Deng, Y. Li, Inorg. Chem. 40 (2001) 5210.
[5] G.J.deA.A. Soler-Illia, A. Louis, C. Sanchez, Chem. Mater. 14 (2002) 750.
[6] J.C. Yu, L. Zhang, J. Yu, New J. Chem. 26 (2002) 416.
[7] K.S. Yoo, T.G. Lee, J. Kim, Micropor. Mesopor. Mater. 84 (2005) 211.
[8] C. Su, C.M. Tseng, L.F. Chen, B.H. You, B.C. Hsu, S.S. Chen, Thin Solid Films 498 (2006) 259.
[9] J. Jiao, Q. Xu, L. Li, J. Colloid Interface Sci. 316 (2007) 596.
[10] H.X. Li, Z.F. Bian, J. Zhu, D.Q. Zhang, G.S. Li, Y.N. Huo, H. Li, Y.F. Lu, J. Am. Chem. Soc. 129 (2007) 8406.
[11] P. Li, K. de Groot, J. Sol–Gel Sci. Technol. 2 (1994) 797.
[12] S. Bu, Ch. Cui, X. Liu, L. Bai, J. Sol–Gel Sci. Technol. 43 (2007) 151.
[13] M. Woodhouse, B.A. Parkinson, Chem. Mater. 20 (2008) 2495.
[14] N. Arconada, A. Durán, S. Suárez, R. Portela, J.M. Coronado, B. Sánchez, Y. Castro, Appl. Catal. B: Environ. 86 (2009) 1.
[15] K. Kajihara, T. Yao, J. Sol–Gel Sci. Technol. 17 (2000) 173.
[16] K. Kajihara, K. Nakanishi, K. Tanaka, K.K. Hirao, N. Soga, J. Am. Ceram. Soc. 81 (1998) 2670.
[17] T. Miki, K. Nishizawa, K. Suzuki, K. Kato, Mater. Lett. 58 (2004) 2751.
[18] K. Kajihara, K. Nakanishi, J. Mater. Res. 16 (2001) 58.
[19] S. Bu, Z. Jin, X. Liu, L. Yang, Z. Cheng, Mater. Chem. Phys. 88 (2004) 273.
[20] M. Arpi, B. Subhayan, H.M. Faruk, T. Takakazu, J. Phys. 100 (2008) 012006.
[21] J.C. Yu, J. Yu, H.Y. Tang, L. Zhang, J. Mater. Chem. 12 (2002) 81.
[22] Y. Paz, A. Heller, J. Mater. Res. 12 (10) (1997) 2759.
[23] P. Dzik, M. Veselý, J. Chomoucká, J. Adv. Oxid. Technol. 13 (2010).
[24] Y. Han, D. Chen, J. Sun, Y. Zhang, K. Xu, Acta Biomater. 4 (2008) 1518.
[25] T. Watanabe, A. Nakajima, R. Wang, M. Minabe, S. Koizumi, A. Fujishima, K. Hashimoto, Thin Solid Films 351 (1999) 260.
[26] T. Zubkov, D. Stahl, T.L. Thompson, D. Panayotov, O. Diwald, J.T. Yates Jr., J. Phys. Chem. B 109 (2005) 15454.
[27] J. Yu, X. Zhao, Q. Zhao, G. Wang, Mater. Chem. Phys. 68 (2001) 253.
[28] V. Brezova, M. Ceppan, M. Vesely, L. Lapcik, Chem. Pap. 45 (1991) 233.
[29] D.F. Ollis, Environ. Sci. Technol. 19 (1985) 480.
[30] R.W. Matthews, J. Chem. Soc. Faraday Trans. 1 85 (1989) 1291.
[31] B. Ohtani, Chem. Lett. 37 (2008) 217.
[32] H. Kisch, W. Macyk, ChemPhysChem 3 (2002) 399.
[33] J. Ryu, W. Choi, Environ. Sci. Technol. 42 (2008) 294.